

CRACK ARREST IN TITANIUM ALLOY: NUMERICAL AND EXPERIMENTAL STUDY

N. Bonora <sup>1</sup>, D. Gentile <sup>2</sup>, M. Marchetti <sup>2</sup>, P.P. Milella <sup>3</sup> and A. Pini <sup>3</sup>

Crack propagation and arrest is one of the main research topic for those materials that are widely used in the aerospace, nuclear and off-shore engineering. Getting more information about the possibility to arrest a dynamic propagating crack gives a broad view of the phenomena related to the crack propagation and is an important step to develop safety criteria. In the present paper the results of experimental work on the determination of the crack-arrest toughness in Ti-6Al-4V are presented. Two different geometry specimens were investigated in order to perform crack arrest tests on this alloy.

In addition, a numerical simulation and analysis of the crack propagation process was performed on both the geometries using a finite element code developed for this specific application.

### INTRODUCTION

The fact that a crack propagating into a continuum can arrest is definitely not new. Many experimental and theoretical studies were performed to determine the arrest condition of a fast running crack in a homogeneous material (1-7). Many of the works on this subject are focused on the arrest capability of steels but very few works investigated this mechanism in other materials. The behaviour of the crack arrest process changes substantially with the material properties so that in some cases, as for the Al alloy (9), the conditions necessary for a fast running crack and for its possible arrest are drastically different. Today the only standard available to measure crack arrest fracture toughness ( $K_{Ia}$ ) in metallic materials is related to ferritic steel and is covered by ASTM E 1221-88 (8).

The requirements provided by the ASTM E 1221-88 standard are very tight and, in many cases, they do not allow to get valid  $K_{Ia}$  measurements for different metals as Al and Ti based alloys. Nevertheless, since no other standards were available, the crack arrest fracture toughness of the Ti alloy was measured using the ASTM E 1221-88 standard procedure.

The specimen geometry strongly affects the possibility to have a fast crack propagation and to obtain a valid measurement of the toughness at the arrest. In order to generate a fast running

- 1 Dip. Ingegneria Industriale, Univ. of Cassino - Via Zamosch 43, 03043 Cassino (FR), Italy
- 2 Aerospace Dept., Univ. of Rome "La Sapienza" - Via Eudossiana 18 - 00184 Rome, Italy
- 3 ENEA-DISP - Via Branconi 48 - 00144 Roma

crack in a Ti alloy used for aerospace applications, a new specimen geometry, previously studied (9) for Al alloy and called WLTC (Wedge Leaded Tapered Crack Arrest Specimen), was investigated in addition to the standard specimen, usually referred as CCA (Compact Crack Arrest), suggested in the ASTM E 1221-88.

An extensive experimental work was performed in order to measure the arrest fracture toughness, at room temperature, of Ti-6Al-4V alloy. The effect of the specimen geometry on the measured values of  $K_{Ia}$  was evaluated using the finite element code SPACCA (10), developed to study the dynamic crack propagation in both the elastic and the plastic regime. Tab. 1 reports material data related to the selected Ti alloy.

TABLE 1 – Material property

$\sigma_r = 895 \text{ MPa};$	$\sigma_y = 825 \text{ MPa};$	elongation 10%
hardner = 36-39 HCR;	$E = 115 \text{ GPa};$	density = $4.43 \text{ g/cm}^3$

FEM Analysis

The ASTM E 1221-88 standard provides the equation that relates the applied stress intensity factor  $K_I$  to the edge displacement  $\delta$  of the crack arrest specimen

$$K_I = \delta E \sqrt{\frac{B}{B_n W}} f\left(\frac{a}{W}\right) \tag{1}$$

where B is the specimen thickness,  $B_n$  the specimen thickness reduced by side grooves, E the Young modulus, W the specimen width and  $f(a/W)$  the shape function that takes into account the specimen geometry and the crack depth a (fig. 1).

Different specimen geometries require different shape functions. The shape function can be determined numerically. A finite Element Method (FEM) analysis of the specimen allows to calculate  $K_I$  values for different crack depths, assuming a fixed edge displacement  $\delta$ .

Previous studies (9) showed that the CCA specimen could not be appropriate to evaluate  $K_{Ia}$  for metals different from ferritic steels. In alternative to the CCA specimen a different geometry was used.

The WLTC is a crack arrest specimen with a geometry that allows to have a K distribution as function of the crack depth "a" different from the CCA specimen. The difference is due to the effect of the increasing material sections involved. The use of this geometry required, as a first step, the determination of a new shape function. In order to verify the code performance, a numerical analysis was performed evaluating the shape function for the CCA specimen and comparing the calculated function with the one suggested by ASTM. The code used for this calculations is the finite element code, SPACCA (10), that allows also the follow the dynamic crack propagation and to estimate the value of the  $K_{Ia}$  and the final crack extension, in both the elastic and the plastic regime. Fig. 2 shows the comparison between the  $f(a/W)$  curve computed by FEM and the  $f(a/W)$  values given in (8). The agreement between the two curves in fig. 2 is very good, particularly if it is taken into account that the mesh used is not very refined and the number of degrees of freedom is limited. 8 node and 6 node triangular bi-linear elements were used in plane strain formulation.

Fig 4 shows  $K_I$  values as function of a/W for the CCA specimen (CCA curve). The slope of the

K(a/W) curve is very steep, suggesting a rapid arrest of a running crack within a very short distance, for a material that exhibits a low fracture toughness  $K_{Ic}$ . This is the case for the Ti alloy. Using such a material the final crack depth could be too small to be taken as a valid result according to the ASTM standard. This is the reason why the WLTCa specimen was developed. The  $K_I$  trend as function of a a/W for WLTCa is reported in fig. 4 for comparison to the corresponding trend in the CCA specimen. The slope of the curve in the case of the WLTCa specimen is smoother. The effect is a larger crack growth before the arrest. The numerical simulation allowed to confirm, at least from the theoretical point of view, the possibility to perform a valid crack arrest test, at room temperature, using Ti alloy.

### EXPERIMENTAL TESTS

The loading system used is the same as prescribed by the ASTM E 1221-88 standard. The specimen is set on a rigid horizontal plane. The load is applied by means of a wedge that is pushed through a circular hole, vertically to the specimen plane. In this way, the hole surfaces through the thickness see an increasing pressure due to the variation of the wedge profile. Such a loading device imposes a force (N), in the plane of the specimen, that opens the two specimen wings.

During the test the vertical load (P), applied on the wedge, and the specimen edge opening  $\delta$  are monitored. Fig. 5 shows an example of the load-displacement plots obtained during the tests. Several loading cycles are necessary to avoid large plastic strain at the tip of the crack. Each loading cycle is characterized by an increasing load phase followed by a constant displacement load drop, corresponding to the reversal of the wedge motion, and by a decreasing load phase.

Once the crack starts the load drops very quickly up to the moment when the crack stops. A new loading ramp helps to mark properly the arrest point. The measured slope in this last loading ramp is different by the previous one because of the crack growth. The values of the load when the crack starts ( $P_0$ ) and arrests ( $P_a$ ), along with the crack length measurement, are used to calculate the values of the toughness at the crack initiation ( $K_{I0}$ ) and at its arrest ( $K_{Ia}$ ), using equation (1). Tab. 2 reports the results of nine tests. For each test the crack propagation  $\Delta a$ , the initiation and arrest loads ( $P_0$ - $P_a$ ) and the initiation and arrest calculated fracture toughness ( $K_{I0}$ - $K_{Ia}$ ) are reported. Tests were performed both in the longitudinal (1-4-9) and in the transverse direction.

The toughness values measured for each specimen are plotted in fig. 6. The mean values are 110 MPa $\sqrt{m}$  for  $K_{I0}$  and 89 MPa $\sqrt{m}$  for the  $K_{Ia}$ . These values are very consistent with the fracture toughness values given in the literature (106 MPa  $\sqrt{m}$ ) for  $K_{Ic}$ .

Crack length measurement is a critical point in this kind of tests, especially when the crack propagates out of plane or it takes the characteristic "nail shape". In order to measure properly the crack growth both dye penetrant and exposure at high temperature were used. Fig. 7 reports the  $K_{Ia}$  values as function of the measured crack propagation. Specimen n. 8 is the only one that had a propagation (11 mm) that is not sufficient to consider the test valid according to the ASTM E 1221-88. The mean value of crack propagation is approximately 22 mm.

The value of N, the force that opens the specimen in its plane, is not measured and not necessary for  $K_I$  calculations. Anyway it is possible to infer the value of N from the measured P (11) through the equation:

$$N = \frac{P}{2 \operatorname{tg}(\alpha + \beta)} \quad (2) \quad \text{where } \beta \text{ is the friction angle given by: } \beta = \frac{P}{2P - \Delta P} \alpha \quad (3)$$

TABLE 2 – Experimental results

Specimens	$\Delta a$ (mm)	$P_0$ (kN)	$P_a$ (kN)	$K_{I0}$ (MPa m <sup>1/2</sup> )	$K_{Ia}$ (MPa m <sup>1/2</sup> )
WL 1	23	11	8.3	112	91
WT 2	20	12.3	8.1	100	81
WT 3	18	12	8.2	96	78
WL 4	21	11	8.3	106	83
WT 5	29	12.6	6.1	125	100
WT 6	25	12.6	5.6	131	105
WT 7	25	12.24	7.2	110	89
WT 8	11	12.8	7.1	101	85
WL 9	24	13.1	8	116	94

where  $\alpha$  is the wedge semi-angle,  $\Delta P$  is the load drop during each cycle at reversal of wedge motion. Fig. 8 shows a comparison between P and N values for the 9 specimens tested. It is possible to observe a load amplification, due to the wedge profile, by a factor ranging from 3 to 4.

### CONCLUSIONS

Nine specimens made from Ti alloy were tested to measure fracture toughness at initiation and arrest. The experimental and analytical work showed that it is possible to perform crack arrest tests on Ti alloys using the same procedure used for ferritic steel but with a modified specimen geometry. This kind of tests can be performed using machines of limited power and small specimens.

Furthermore this technique allows to measure the crack arrest toughness without a very sensitive or complex data acquisition system.

Acknowledgements - This work has been sponsored by MURST and CNR.

### REFERENCES

- (1) A.R. Rosenfield, P.P. Milella et al. - "Critical Experiments, Measurements and Analyses to Establish a Crack Arrest Methodology for Nuclear Pressure Vessel Steels" - Battelle Columbus Laboratories, Ohio U.S.A..
- (2) R.G. Hogland, A.R. Rosenfield, P.C. Gehelen and G.T. Hahn. - "A Crack Arrest Measuring Procedure for K<sub>I</sub>m, K<sub>ID</sub>, and K<sub>Ia</sub> Properties" - in Fast Fracture and Crack arrest, ASTM STP 627 G.T. Hahn and M.F. Kanninen, Eds., American Society for Testing and Materials.
- (3) L. Dahlberg, F. Nilsson and B. Brickstad - "Influence of specimen geometry on crack propagation and arrest toughness" - in Crack Arrest Methodology and Application, ASTM STP 711, G.T. Hahn and M.F. Kanninen, Eds., American Society for Testing and Materials.

- (4) P.N.R. Keegestra, J.L. Head, C.E. Turner - "A two dimensional dynamic linear-elastic finite element program for the analysis of unstable crack propagation and arrest" - Numerical Methods in Fracture Mechanics.
- (5) G. Rydholm, B. Fredriksson, F. Nilsson - "Numerical investigations of rapid crack propagation" - Numerical Methods in Fracture Mechanics.
- (6) J.F. Malluck, W.W. King - "Fast fracture simulated by conventional finite elements e comparison of two energy-release algorithms" - ASTM STP 711.
- (7) A. Lundberg, L.P. Bryne - "Measurement of rapid crack growth whit ultrasonic transducer" - NBS, Gaithesburg U.S.A..
- (8) ASTM E 1221 88 - "Test Method for Determining the Plane-Strain Crack Arrest Fracture Toughness  $K_{Ia}$  of Ferritic Steels" - 1998, Annual Book of ASTM Standards, American Society for Testing and Materials, Philadelphia, U.S.A..
- (9) M. Marchetti, A. Torelli, P.P. Milella, A. Pini - "Crack Propagation and Arrest in aluminum alloy for Aerospace use" - 17° MPA seminar, 10-11 Oct. 1991 Stuttgart.
- (10) C. Lussu, C. Sampietri - "Studio della propagazione dinamica di cricche in strutture bidimensionali in campo elasto-plastico: il programma SpaccaP." - Rapporto finale CISE 2931 del 06/03/1986.
- (11) M. Barra Carracciolo, P.P. Milella, A. Pini, M. Trafficante - "Calibrazione sperimentale della cedevolezza di un provino compact crack arrest attraverso l'uso del metodo dell'attrito" - IV Congresso Nazionale IGF 26-27 May 1988 Milano.

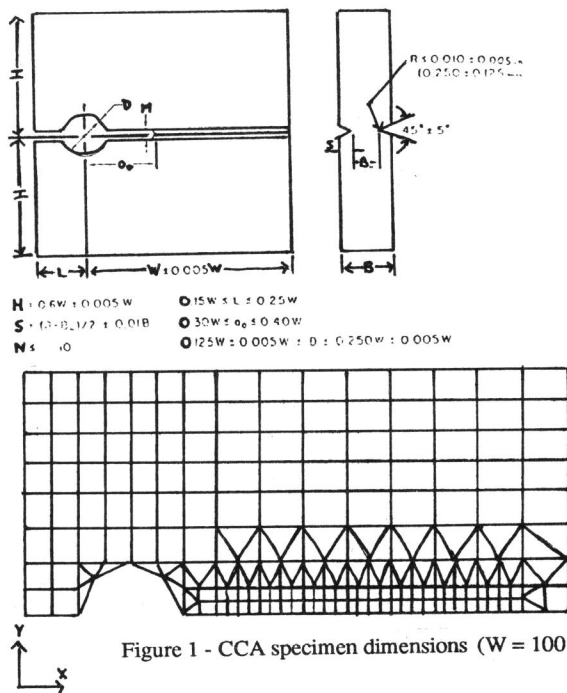


Figure 1 - CCA specimen dimensions ( $W = 100$  mm,  $L = 25$  mm,  $H = 10$  mm).

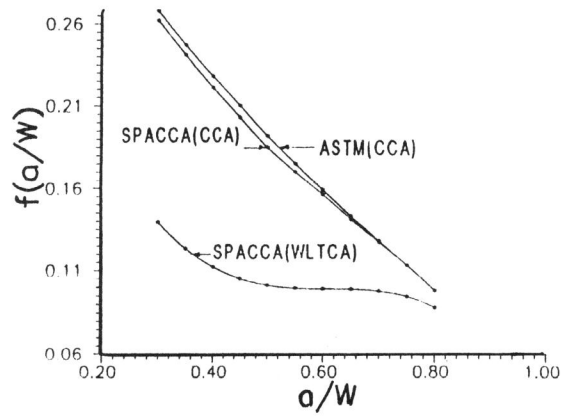


Figure 2 - Comparison between calibration functions for the CCA and WLTCAspecimens.

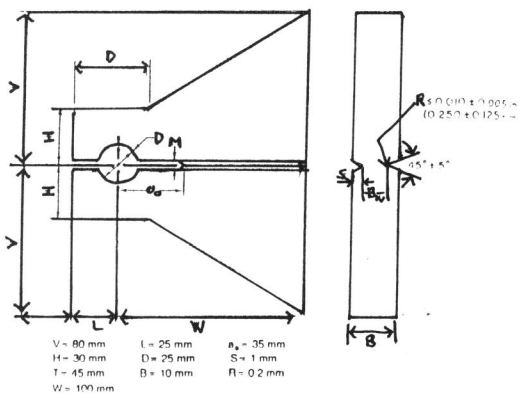
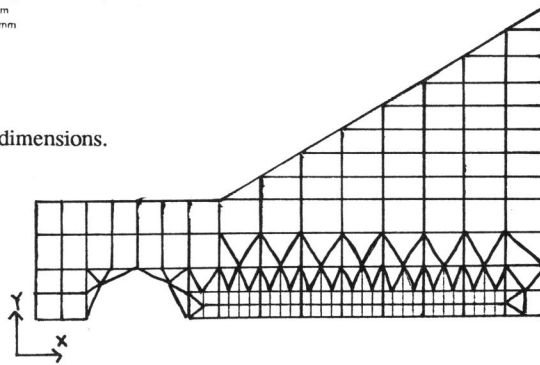


Figure 3 - WLTCAspecimen dimensions.



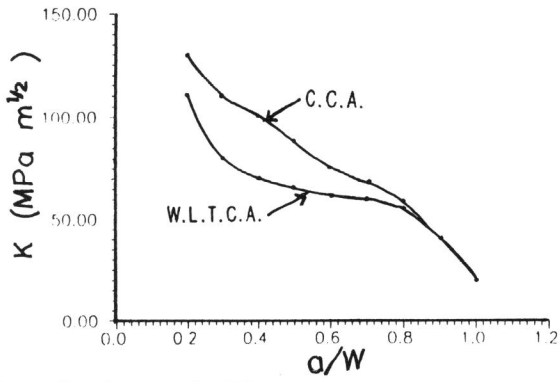


Figure 4 - Comparison between the CCA and the WLTCA  $K_I$  profiles, for an imposed edge opening equal to 1 mm.

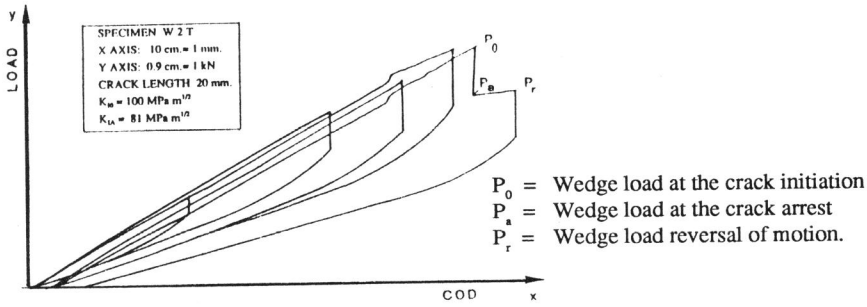


Figure 5 - Experimental test plot of W 2 T specimen.

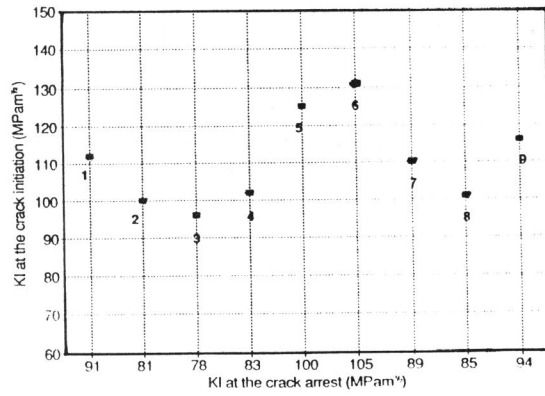


Figure 6 - Comparison between experimental values of  $K_{I0}$  and  $K_{Ia}$ .

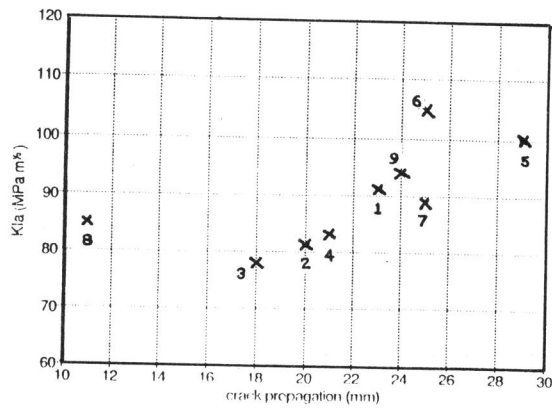


Figure 7 - Experimental result:  $K_{Ia}$  versus ship crack propagation.

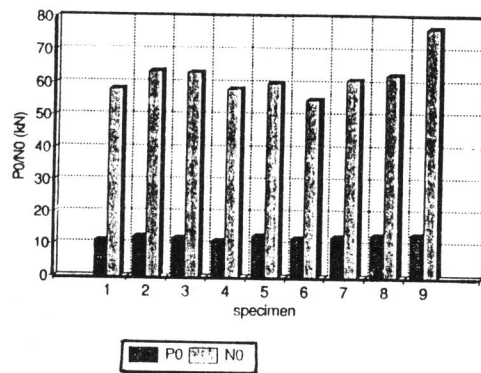


Figure 8 - Comparison between P and N values for the nine tests.

$P_0$  = Wedge load at the crack initiation  
 $N_0$  = Opening load in the specimen plane, crack initiation (see equation 2)